Johann Radon Institute for
Computational and Applied Mathematics
Austrian Academy of Sciences (ÖAW)

On the Adaptive Coupling of Finite Elements and Boundary Elements for Elasto-Plastic Analysis

W. Elleithy, R. Grzhibovskis

RICAM-Report 2008-26

On the Adaptive Coupling of Finite Elements and Boundary Elements for Elasto-Plastic Analysis*

Wael Elleithy[1] **and Richards Grzhibovskis**[2]

[1] Institute of Computational Mathematics, Johannes Kepler University Linz
Altenberger Str. 69, A-4040 Linz, Austria
E-mail address: wael.elleithy@numa.uni-linz.ac.at

[2] Applied Mathematics, University of Saarland, Saarbrücken, Germany
E-mail address: richards@num.uni-sb.de

Abstract

The purpose of this paper is to present an adaptive FEM-BEM coupling method that is valid for both two- and three-dimensional elasto-plastic analyses. The method takes care of the evolution of the elastic and plastic regions. It eliminates the cumbersome of a trial and error process in the identification of the FEM and BEM sub-domains in the standard FEM-BEM coupling approaches. The method estimates the FEM and BEM sub-domains and automatically generates/adapts the FEM and BEM meshes/sub-domains, according to the state of computation. The results for two- and three- dimensional applications in elasto-plasticity show the practicality and the efficiency of the adaptive FEM-BEM coupling method.

Keywords: FEM; BEM; Adaptive Coupling; Elasto-Plasticity

1. Introduction

In many application contexts, coupling of the finite element method (FEM) and the boundary element method (BEM) is, in principle, very attractive. Examples include, but not limited to, elasto-plastic applications with limited spread of plastic deformations (local non-

* The support of the Austrian Science Fund (FWF), Project number: M950, Lise Meitner Program, is gratefully acknowledged. The authors wish to thank Prof. U. Langer Johannes Kepler University Linz, and Prof. S. Rjasanow, University of Saarland for the fruitful discussions and their comments, suggestions and encouragement of this work. Special thanks go to Prof. O. Steinbach, Graz University of Technology, for providing the symmetric Galerkin boundary element computer code utilized in some parts of this investigation. The second author gratefully acknowledges the funding of the German Research Foundation (DFG project SPP-1146).

linearities are only concentrated in a portion of the bounded/unbounded domain). The FEM is utilized where the plastic material behavior is expected to develop. The remaining bounded/unbounded linear elastic regions are best approximated by the BEM.

Since the work of Zienkiewicz and his coauthors [1,2] in coupling of the finite element and boundary element methods, a large number of papers devoted to the topic have appeared (see, e.g., references [3-29] and the literature cited therein).

The symmetric coupling of BEM and FEM goes back to Costabel [3,4]. With the Symmetric Galerkin BEM, FEM-like stiffness matrices can be produced which are suitable for FEM-BEM coupling, see, e.g., references [5,9,12,15,18,19,26]. Brink et al. [10] investigated the coupling of mixed finite elements and Galerkin boundary elements in linear elasticity, taking into account adaptive mesh refinement based on a posteriori error estimators. Carstensen et al. [11] presented an *h*-adaptive FEM-BEM coupling algorithm (mesh refinement of the boundary elements and the finite elements) for the solution of viscoplastic and elasto-plastic interface problems. Mund and Stephan [14] derived a posteriori error estimates for nonlinear coupled FEM-BEM equations by using hierarchical basis techniques. They presented an algorithm for adaptive error control, which allows independent refinements of the finite elements and the boundary elements.

In boundary element analysis, Astrinidis et al. [30] presented adaptive discretization schemes that are based on a stress smoothing error criterion in the case of two-dimensional elastic analysis, and on a total strain smoothing error criterion in the case of two-dimensional elasto-plasticity. Maischak and Stephan [31] showed convergence for the boundary element approximation, obtained by the *hp*-version, for elastic contact problems, and derived a posteriori error estimates together with error indicators for adaptive *hp*-algorithms.

A central aspect of the existing (standard) FEM-BEM coupling approaches is that they require the user/analyst to predefine and manually localize the FEM and BEM sub-domains (prior to analysis). In an elasto-plastic analysis, it is difficult to predict regions where plasticity occurs. If the FEM sub-domain is not predefined so, that it encloses the evolutional plastic regions, significant errors will be introduced to the conducted FEM-BEM coupling analysis. On the other hand, if the FEM sub-domain is notably over-estimated, the excessive number of degrees of freedom (in order to model the linear elastic part) will significantly increase the computational demand.

Doherty and Deeks [32] developed an adaptive approach for analyzing 2D elasto-plastic unbounded media by coupling the FEM with the scaled boundary finite element method.

The analysis begins with an “initial” finite element mesh that tightly encloses the load-medium interface, whereas the remainder of the problem is modeled using the semi-analytical scaled boundary finite element method. Load increments are applied, and if plasticity is detected in the outer band of finite elements, an additional band is added around the perimeter of the existing mesh. The scaled boundary finite element sub-domain is stepped out accordingly. However, this approach requires, in general, a preliminary knowledge of the parts of the domain that are likely to yield. Moreover, it requires additional iterations when plasticity is detected in the outer band of finite elements in order to accurately determine the computational sub-domains.

In boundary element analysis, Rebeiro et al. [33] developed a pure BEM procedure to automatically generate the internal cells to compute domain integrals in the plastic region. The discretization of the internal cells progressively generated only in the regions where plasticity occurs.

Elleithy [29] and Elleithy and Langer [34,35] presented adaptive FEM-BEM coupling algorithms for two-dimensional elasto-plastic analysis. In order to give fast and helpful estimation of the FEM and BEM sub-domains, they proposed the use of simple, and at the same time fast, post-calculations based on energetic methods [36-42], which follows simple hypothetical elastic computations.

This paper presents an adaptive FEM-BEM coupling method that improves and enhances the estimation of regions where plastic material behavior is going to develop (for both two- and three-dimensional elasto-plastic analyses). In order to enable fast and efficient computations for three-dimensional problems, data-sparse boundary element methods are utilized, i.e., Ḥ-matrix representation via Adaptive Cross Approximation (ACA), see, e.g., references [43,44] and the literature cited therein.

An outline of the paper is as follows. In order to make the present article self-contained, Section 2 briefly summarizes the symmetric Galerkin and data-sparse BEM in linear elasticity, FEM in elasto-plasticity, conventional (direct) and interface relaxation FEM-BEM coupling equations, and a brief description of the adaptive coupling algorithms presented in [29,34,35]. Section 3 presents the proposed adaptive FEM-BEM coupling method for elasto-plastic analysis. In Section 4, we present two- and three-dimensional applications in elasto-plasticity that highlights the effectiveness of the adaptive coupling method.

2. Preliminaries

2.1 Symmetric Galerkin and data-sparse BEM in linear elasticity

Advantages of the symmetric Galerkin boundary element method, such as high accuracy and relatively low number of unknowns, make it attractive when solving linear elasticity problems. The formulation of the method together with several applications can be found in references [45, 46, 47, 48, 50]. Although, the number of unknowns is smaller than in the case of a finite element formulation, discretizations of boundary integral operators results in a fully populated system matrix. This renders it prohibitively expensive in terms of storage and numerical complexity when the problem size is large. Approximating the actions of integral operators using multipole expansion and fast summation methods dramatically reduces the complexity and storage requirements (see reference [51]). Another way to accelerate the method is to approximate the fully populated matrices by blockwise low-rank ones (references [43, 44]). In what follows, we formulate the symmetric Galerkin BEM for the linear elasticity problem with mixed boundary conditions, and explain how the solution procedure is accelerated by means of the blockwise low-rank approximation. Material of this section follows references [43, 44].

Let $\Omega \subset \mathsf{R}^n \, (n = 2, 3)$ be a bounded domain with a Lipschitz boundary $\Gamma = \partial\Omega$. We consider a mixed boundary value problem in linear elasticity, to determine the displacement field $\underline{u}(x) \in \mathsf{R}^n$ for $x \in \Omega$, satisfying

$$\begin{aligned} -\sigma_{ij,j}(\underline{u}, x) &= 0 && \text{for } x \in \Omega, \\ u_i(x) &= g_i(x) && \text{for } x \in \Gamma_D, \\ t_i(x) = \sigma_{ij}(u)\, n_j(x) &= w_i(x) && \text{for } x \in \Gamma_N. \end{aligned} \tag{1}$$

The stress tensor $\sigma_{ij}(u)$ is related to the strain tensor

$$\varepsilon(\underline{u}) = \frac{1}{2}(\nabla \underline{u}^T + \nabla \underline{u}), \tag{2}$$

by Hooke's law

$$\sigma(\underline{u}) = \frac{E\nu}{(1+\nu)(1-2\nu)}\left[\operatorname{tr} \varepsilon(\underline{u}) I + \frac{E}{(1+\nu)}\varepsilon(\underline{u})\right]. \tag{3}$$

The *i*-th boundary stress vector component is given by the operator $(T_x \underline{u}(x))_i = \sigma_{ij}(\underline{u}, x) n_j(x)$ where $\underline{n}(x)$ is the outward normal vector defined for almost all $x \in \Gamma$. For isotropic elastostatics and assuming a homogeneous material behavior with

constant parameters (Young modulus E and Poisson ratio ν), the first (weakly singular) boundary integral equation can be written as

$$\int_{\Gamma} U^*(x,y)\,\underline{t}\,(y)\,ds_y = \frac{1}{2}\underline{u}\,(x) + \int_{\Gamma} T^*(x,y)\,\underline{u}\,(y)ds_y, \tag{4}$$

where $T^*(x,y) = (T_y U^*(x,y))^{\mathrm{T}}$ for $y \in \Gamma$. The fundamental solution $U_{ij}^*(x,y)$ of the Lame system (1) is given by the Kelvin tensor

$$U_{ij}^*(x,y) = \frac{1}{4(n-1)\,\pi}\frac{1}{E}\frac{1+\nu}{1-\nu}\left[(3-4\nu)Z(x,y)\delta_{ij} + \frac{(x_i-y_i)(x_j-y_j)}{|x-y|^n}\right], \tag{5}$$

where $i,j = 1,....,n$, $|x-y|$ denotes the Euclidean distance between the source and field points, $Z(x,y) = -log|x-y|$ for $n=2$ and $Z(x,y) = \dfrac{1}{|x-y|}$ for $n=3$.

In the symmetric formulation we further use the second (hypersingular) boundary integral equation [45,46,50,51]

$$-T_x\int_{\Gamma} T^*(x,y)\,\underline{u}\,(y)ds_y = \frac{1}{2}\underline{t}\,(x) - \int_{\Gamma} T_x U^*(x,y)\,\underline{t}\,(y)ds_y. \tag{6}$$

Corresponding to the boundary integral equations (4) and (6), the standard notations for the boundary integral operators V, K, K' and D (the single layer potential, double layer potential, its adjoint and hypersingular integral operators, respectively) are given by

$$\begin{aligned}
(V\underline{t})(x) &= \int_{\Gamma} U^*(x,y)\,\underline{t}\,(y)ds_y,\\
(K\underline{u})(x) &= \int_{\Gamma} T^*(x,y)\,\underline{u}\,(y)ds_y,\\
(K'\underline{t})(x) &= \int_{\Gamma} T_x U^*(x,y)\,\underline{t}\,(y)ds_y,\\
(D\underline{u})(x) &= -T_x\int_{\Gamma} T^*(x,y)\,\underline{u}\,(y)ds_y.
\end{aligned} \tag{7}$$

In order to find the complete Cauchy data $[\underline{u},\underline{t}]_{\Gamma}$, the first integral equation (4) is used where the traction $\underline{t}$ is unknown [45,46,50,51]

$$(V\underline{t})(x) = \frac{1}{2}\underline{g}\,(x) + (K\underline{u})\,(x) \quad \text{for } x \in \Gamma_D, \tag{8}$$

whereas the second boundary integral equation (6) is used where the displacement $\underline{u}$ is unknown [45,46,50,51]

$$(D\underline{u})(x)=\frac{1}{2}\underline{w}(x)-(K'\underline{t})(x) \text{ for } x\in\Gamma_N. \tag{9}$$

Now let us denote by $\underline{\tilde{g}}$ and $\underline{\tilde{w}}$ arbitrary extensions of the given Dirichlet $\underline{g}$ and Neumann data $\underline{w}$, respectively, such that $\underline{\tilde{g}}(x)=\underline{g}(x)$ for $x\in\Gamma_D$ and $\underline{\tilde{w}}(x)=w(x)$ for $x\in\Gamma_N$. With the splitting of the Cauchy data into the unknown and known parts $\underline{u}(x)=\underline{\tilde{u}}(x)+\underline{\tilde{g}}(x)$ and $\underline{t}(x)=\underline{\tilde{t}}(x)+\tilde{w}(x)$, only the unknown functions $\underline{\tilde{u}}(x)$ and $\underline{\tilde{t}}(x)$ have to be determined. Then the variational formulation leads to finding $\underline{\tilde{u}}(x)$ and $\underline{\tilde{t}}(x)$ such that

$$(V\underline{\tilde{t}})(x)-(K\underline{\tilde{u}})(x)=\frac{1}{2}\underline{\tilde{g}}(x)+K\underline{\tilde{g}}(x)-V\underline{\tilde{w}}(x) \text{ for } x\in\Gamma_D, \tag{10}$$

$$(K'\underline{\tilde{t}})(x)+(D\underline{\tilde{u}})(x)=\frac{1}{2}\underline{\tilde{h}}(x)-(K'\underline{\tilde{w}})(x)-(D\underline{\tilde{g}})(x) \text{ for } x\in\Gamma_N. \tag{11}$$

The standard Galerkin discretization of (10) and (11) using anzats

$$\underline{\tilde{u}}^h(x)=\sum_{j=1}^{N'}\underline{u}_j\psi_j(x), \quad \underline{\tilde{t}}^h(x)=\sum_{i=1}^{N}\underline{t}_i\varphi_i(x), \tag{12}$$

yields the skew-symmetric and positive definite system of linear equations

$$\begin{pmatrix} V_h & -K_h \\ K_h^T & D_h \end{pmatrix}\begin{pmatrix} \underline{\tilde{t}}^h \\ \underline{\tilde{u}}^h \end{pmatrix}=\begin{pmatrix} \underline{f}_1 \\ \underline{f}_2 \end{pmatrix}, \tag{13}$$

where h is the discretization parameter, N is the number of boundary elements, N' is the number of boundary nodes, $\psi_j(x)$ are the piecewise linear nodal basis functions, $\varphi_i(x)$ are piecewise constant element basis functions, $\underline{u}_j$ and $\underline{t}_i$ are vector valued partially unknown coefficients. The matrices in (13) consist of the following elements

$$(V_h)_{kl}=\left\langle V\underline{\varphi}_l,\underline{\varphi}_k\right\rangle_{\Gamma_D}, \quad (K_h)_{kj}=\left\langle K\underline{\psi}_j,\underline{\varphi}_k\right\rangle_{\Gamma_D}, \quad (D_h)_{ij}=\left\langle D\underline{\psi}_j,\underline{\psi}_i\right\rangle_{\Gamma_N}, \tag{14}$$

where $\underline{\varphi}_i=(\varphi_i,\varphi_i,\varphi_i)^T$ and $\underline{\psi}_i=(\psi_i,\psi_i,\psi_i)^T$.The right hand side vectors $\underline{f}_1$ and $\underline{f}_2$ result from discretization of the corresponding right hand sides of (10) and (11).

In typical applications in linear elastostatics, the Dirichlet part Γ_D is often smaller than the Neumann part Γ_N where the boundary tractions are prescribed. Therefore, the inverse of the discrete single layer potential V_h may be computed using some direct method such as a Cholesky decomposition to obtain

$$\underline{\tilde{t}}^{h} = V_h^{-1}[\underline{f}_1 + K_h \underline{\tilde{u}}^{h}]\cdot \tag{15}$$

Inserting (15) into the second of (13) yields the Schur complement system

$$[D_h + K_h^T V_h^{-1} K_h]\,\underline{\tilde{u}}^{h} = \underline{f}_2 - K_h^T V_h^{-1}\,\underline{f}_1\cdot \tag{16}$$

The Schur complement system (16) is symmetric and positive definite and is suitable for coupling with FEM. System (16) may be rewritten as

$$[{}_B K][{}_B \underline{u}] = [{}_B \underline{f}], \tag{17}$$

where the subscript *B* stands for the BEM sub-domain.

When treating three dimensional problems, however, the number of degrees of freedom can be large, and one has to avoid explicit generation of the fully populated matrices (14). To do so, we perform the following steps (see also reference [43]):

1. rewrite expressions for $\langle K\underline{u},\underline{t}\rangle, \langle K'\underline{t},\underline{u}\rangle$ and $\langle D\underline{u},\underline{u}\rangle$ using integration by parts,
2. renumber degrees of freedom and approximate matrices by blockwise low-rank.

As it was shown in [52] (see also [44,51]) the action of K and K' can be expressed in terms of V, V_L, K_L, and R

$$\begin{aligned}\langle K\underline{u},\underline{t}\rangle &= 2\mu\langle VR\underline{u},\underline{t}\rangle + \langle K_L\underline{u},\underline{t}\rangle - \langle V_L R\underline{u},\underline{t}\rangle,\\ \langle K'\underline{t},\underline{u}\rangle &= 2\mu\langle V\underline{t},R\underline{u}\rangle + \langle K_L'\underline{t},\underline{u}\rangle - \langle V_L\underline{t},R\underline{u}\rangle,\end{aligned} \tag{18}$$

where V_L, K_L are the corresponding operators for the Laplace equation

$$(V_L\underline{t})(x) = \frac{1}{4\pi}\int_\Gamma \frac{1}{|x-y|}\underline{t}(y)\,\mathrm{d}s_y, \tag{19}$$

$$(K_L\underline{u})(x) = \frac{1}{4\pi}\int_\Gamma \frac{\partial}{\partial n_y}\left[\frac{1}{|x-y|}\right]\underline{u}(y)\mathrm{d}s_y, \tag{20}$$

where μ is the Lamė constant, $\underline{u}$, $\underline{t}$ are some vector valued functions on Γ, and

$$R_{ij} = n_j\frac{\partial}{\partial x_i} - n_i\frac{\partial}{\partial x_j}. \tag{21}$$

In the same literature, one finds the following formula for the action of the hypersingular operator D

$$\langle D\underline{u},\underline{v}\rangle = \int_\Gamma\int_\Gamma \frac{\mu}{4\pi|x-y|}\left(\sum_{k=1}^{3}\frac{\partial}{\partial S_k}\underline{u}(y)\frac{\partial}{\partial S_k}\underline{v}(x)\right)+$$
$$+(R\underline{v})^T(x)\left(\frac{\mu}{2\pi|x-y|}I-4\mu^2U^*(x,y)\right)(R\underline{u})(y)+ \qquad (22)$$
$$+\sum_{i,j,k=1}^{3}(R_{kj}v_i)(x)\frac{1}{|x-y|}(R_{ki}u_j)(y)\,\mathrm{d}s_x\mathrm{d}s_y.$$

Here $\underline{u}$ and $\underline{v}$ are some vector valued functions on Γ, and

$$\frac{\partial}{\partial S_1}=R_{32},\quad \frac{\partial}{\partial S_2}=R_{13},\quad \frac{\partial}{\partial S_3}=R_{21}. \qquad (22)$$

Using the above expressions, the action of the discretized versions of the boundary integral operators are reduced to several matrix vector products, where the only fully populated matrices are $(V_h)_{kl}$, $(V_{hL})_{kl}$, and $(K_{hL})_{ij}$.

In order to construct a blockwise low-rank approximants to these matrices, we perform a hierarchical renumbering of boundary nodes and elements. This procedure is referred to as clustering, because the nodes and elements are grouped together forming clusters. Any pair of such clusters is represented in the corresponding matrix by a block. The key observation is that if the clusters are well separated, this block has a low-rank approximant, and the Adaptive Cross Approximation (ACA) procedure can be used to find it (see reference [43], where the ACA procedure for Galerkin matrices is discussed). The benefit of using the ACA procedure in combination with the clustering is the reduction of the complexity and storage requirements from $O(N^2)$ to $O(N\log N)$ operations and units, respectively.

2.2 FEM in elasto-plasticity

First let us consider a boundary value problem in linear elasticity. A solid occupying Ω (in which the internal stresses σ, the distributed volume force $\underline{f}$ and the external applied tractions $\underline{w}$ form an equilibrating field) is considered to undergo an arbitrary virtual displacement $\delta\underline{u}$ which results in compatible strains $\delta\varepsilon$ and internal displacements $\delta\underline{d}$. Then the principle of virtual work requires that [53]

$$\int_\Omega \delta\varepsilon^T\sigma d\Omega-\int_\Omega \delta\underline{d}^T\,\underline{f}\,d\Omega-\int_{\Gamma_N}\delta\underline{d}^T\,\underline{w}\,d\Gamma=0. \qquad (23)$$

The normal finite element discretizing procedure leads to the following expressions for the displacements and strains within any element

$$\delta \underline{d} = N \delta \underline{u}, \qquad \delta \underline{\varepsilon} = B \delta \underline{u}, \tag{24}$$

where N and B are the usual matrix of shape functions and the elastic strain-displacement matrix, respectively. The element assembly process gives

$$\int_{\Omega} \delta \underline{u}^T (B^T \sigma - N^T \underline{f}) \, d\Omega - \int_{\Gamma_N} \delta \underline{u}^T N^T \underline{w} \, d\Gamma = 0, \tag{25}$$

where the volume integration over the solid is the sum of the individual element contributions. Since (25) must hold true for any arbitrary $\delta \underline{u}$,

$$\int_{\Omega} B^T \sigma \, d\Omega - (\int_{\Omega} N^T \underline{f} \, d\Omega + \int_{\Gamma_N} N^T \underline{w} \, d\Gamma) = 0. \tag{26}$$

Substituting $\sigma = C\varepsilon$ into (26) we obtain

$$K \underline{u} = (\int_{\Omega} N^T \underline{f} \, d\Omega + \int_{\Gamma_N} N^T \underline{w} \, d\Gamma), \tag{27}$$

where the stiffness matrix is given by $K = \int_{\Omega} B^T C \, B \, d\Omega$. The final system of the assembled finite element equations in elasticity may now be written as

$$[{}_F K][{}_F \underline{u}] = [{}_F \underline{f}], \tag{28}$$

where the subscript F stands for the FEM sub-domain.

Some force terms in (26) may be a function of displacement, u, or stress may be a nonlinear function of strain, ε, as a result of material non-linearity such as plasticity. In all of these cases, a nonlinear solution procedure is required. Equation (26) will not be generally satisfied at any stage of computation, and thus the equilibrium equation can be restated in the form of a residual (or out-of-balance) force vector, $\underline{\psi}$, given by (see references [53,54] for further details on computational aspects)

$$\underline{\psi} = \int_{\Omega} B^T \sigma \, d\Omega - (\int_{\Omega} N^T \underline{f} \, d\Omega + \int_{\Gamma_N} N^T \underline{w} \, d\Gamma) \neq 0. \tag{29}$$

If a material nonlinear-only analysis is performed, the integrals in the above equation are computed with respect to the initial configuration (Lagrangian FEM formulation). For an elasto-plastic situation the material stiffness is continuously varying, and instantaneously the incremental stress-strain relationship is given by

$$d\sigma = D_{ep} \, d\varepsilon, \tag{30}$$

where D_{ep} is the elasto-plastic stress-strain matrix.

The solution procedure involves the incremental form of (29), namely

$$\Delta\underline{\psi} = \int_{\Omega} B^T \Delta\sigma \, d\Omega - (\int_{\Omega} N^T \Delta \underline{f} \, d\Omega + \int_{\Gamma_N} N^T \Delta \underline{w} \, d\Gamma). \tag{31}$$

Substituting (30) into (31) we obtain

$$\Delta\underline{\psi} = K_T \Delta\underline{u} - (\int_{\Omega} N^T \Delta \underline{f} \, d\Omega + \int_{\Gamma_N} N^T \Delta \underline{w} \, d\Gamma), \tag{32}$$

where the tangent stiffness matrix is given by $K_T = \int_{\Omega} B^T D_{ep} B \, d\Omega$.

Equation (32) may now be written as

$$[\Delta\underline{\psi}] = [K_T][\Delta\underline{u}] - [\Delta \underline{f}]. \tag{33}$$

For the solution of (33), and for each load increment consider the situation existing for the r^{th} iteration. The applied loads for the r^{th} iteration are the residual forces $\Delta\underline{\psi}^{r-1}$ calculated at the end of the $(r-1)^{th}$ iteration according to (33). These applied loads give rise to displacement increments $\Delta\underline{u}^r$. The corresponding increments of the strain $\Delta\varepsilon^r$ are calculated. The incremental stress change assuming elastic behavior is computed. The computed stresses are then brought down to the yield surface and are used to calculate the equivalent nodal forces. These nodal forces can be compared with the externally applied loads to form the residual forces for the next iteration. The system of residual forces is brought sufficiently close to zero through the iterative process, before moving to the next load increment.

2.3 Coupled FEM-BEM in elasto-plasticity

Elasto-plastic problems with limited spread of plastic deformations lend themselves to a coupled FEM-BEM approach. The FEM is utilized in regions where plastic material behavior is expected to develop, whereas the complementary bounded/unbounded linear elastic region is approximated using the symmetric Galerkin boundary element method (data-sparse boundary element methods in order to enable fast and efficient computations for three-dimensional applications). For a numerical representation of an arbitrary domain Ω with known boundary conditions specified on the entire boundary $\Gamma = \Gamma_N \cup \Gamma_D$, the FEM (see, Section 2.2) and BEM (see, Section 2.1) are used. The domain is decomposed into two sub-domains, namely ${}_F\Omega$ and ${}_B\Omega$, with the FEM-BEM coupling interface Γ_C.

In the conventional (direct) FEM-BEM coupling methods, the stiffness matrix ${}_BK$ is interpreted as the element stiffness matrix of a finite macro element, computed by the BEM. Combining (17) and (33), while satisfying the continuity conditions along the FEM-BEM interface, results in

$$\begin{bmatrix} \Delta_F \underline{\psi}_F \\ \Delta \underline{\psi}_C \\ \Delta_B \underline{\psi}_B \end{bmatrix} = \begin{bmatrix} {}_FK_{TFF} & {}_FK_{TFC} & \\ {}_FK_{TCF} & {}_FK_{TCC} + {}_BK_{CC} & {}_BK_{CB} \\ & {}_BK_{BC} & {}_BK_{BB} \end{bmatrix} \begin{bmatrix} \Delta_F \underline{u}_F \\ \Delta \underline{u}_C \\ \Delta_B \underline{u}_B \end{bmatrix} - \begin{bmatrix} \Delta_F \underline{f}_F \\ \Delta_B \underline{f}_C + \Delta_F \underline{f}_C \\ \Delta_B \underline{f}_B \end{bmatrix} \cdot \quad (34)$$

where the subscripts $()_F$ and $()_B$ indicate the displacement vectors (force vectors) not associated with the FEM and BEM sub-domains interface, respectively. The subscript $()_C$ indicates those associated with the interface Γ_C. For each load increment, the global equation systems (34) are solved.

As an alternative to the conventional (direct) FEM-BEM coupling methods, a partitioned solution scheme can be used, where the systems of equations of the sub-domains are solved independently of each other. The interaction effects are taken into account as boundary conditions, which are imposed on the coupling interfaces. Iterations are performed in order to enforce satisfaction of the coupling conditions. Within the iteration procedure, a relaxation operator is applied to the interface boundary conditions in order to enable and speed up convergence. In this sense, the iterative coupling approaches are better called interface relaxation FEM-BEM coupling methods [21,23]. The interface relaxation FEM-BEM (Dirichlet-Neumann) coupling method in elasto-plasticity is outlined as:

Set initial guess $({}_F\underline{u}_C)_{n=0}$ (where n is the iteration number).

For $n =$ 1, 2,..., do until convergence

FEM sub-domain:

solve Equation (33) for $({}_F\underline{f}_C)_n$

solve $({}_F\underline{f}_C)_n = [M]({}_F\underline{t}_C)_n$ for $({}_F\underline{t}_C)_n$, where $[M]$ is a converting matrix, which depends on the interpolation functions used to represent the tractions ${}_F\underline{t}_C$ on the interface.

BEM sub-domain:

Set $({}_B\underline{t}_C)_n + ({}_F\underline{t}_C)_n = 0$

Solve Equation (17) for $({}_B\underline{u}_C)_n$

apply $({}_F\underline{u}_C)_{n+1} = (1-\theta)\,({}_F\underline{u}_C)_n + \theta({}_B\underline{u}_C)_n$ where θ is a relaxation parameter to ensure and/or accelerate convergence.

The convergence characteristics of the interface relaxation FEM-BEM coupling methods were studied extensively by Elleithy and co-workers [16,17]. The convergence/optimal convergence of the interface relaxation coupling methods is ensured by properly set relaxation parameters that can be assigned constant values for all iterations. The optimal and applicable ranges of static relaxation parameters may be obtained by experimenting with different values. Alternatively, prior to coupled FEM-BEM calculations, static values of the relaxation parameters may be obtained [16,17]. It requires, however, some sort of intricate matrix manipulations. Optimal dynamic values of the relaxation parameters may be utilized in order to significantly reduce the required number of FEM-BEM coupling iterations [55]. For dynamic calculation of relaxation parameters for the interface relaxation (Dirichlet-Neumann) FEM-BEM coupling method the following relation may be utilized

$$\theta_{n+1} = \frac{\left\| ({}_F\underline{u}_C)_n - ({}_F\underline{u}_C)_{n-1} \right\|_2^2 - (({}_F\underline{u}_C)_n - ({}_F\underline{u}_C)_{n-1}).(({}_B\underline{u}_C)_n - ({}_B\underline{u}_C)_{n-1})}{\left\|(({}_B\underline{u}_C)_n - ({}_B\underline{u}_C)_{n-1}) - (({}_F\underline{u}_C)_n - ({}_F\underline{u}_C)_{n-1})\right\|_2^2}, \qquad (35)$$

where $\|\cdot\|_2$ is Euclidean (l_2) norm.

2.4 Adaptive coupling methods [29,34,35]

References [29,34,35] presented adaptive FEM-BEM coupling methods for solving problems in elasto-plasticity. The algorithms follow linear hypothetical elastic computations at levels of loading specified by the user. The hypothetical elastic state of stresses is checked against yielding with a pseudo value of the material yield strength. An estimate of the regions sensible for FEM discretization is then derived. The FEM and BEM meshes are automatically generated. A coupled FEM-BEM stress analysis involving elasto-plastic deformations is then conducted. In order to determine the pseudo value of the material yield strength, an energy balance between the hypothetical elastic and elasto-plastic calculations was assumed [29,34,35]

$$U_{\text{hyp elastic}} := \left(\int_\Omega \sigma_{ij}\varepsilon_{ij}\,dV\right)_{\text{hyp elastic}} \approx \left(\int_\Omega \sigma_{ij}\varepsilon_{ij}\,dV\right)_{\text{elasto-plastic}}, \qquad (36)$$

where $U_{\text{hyp elastic}}$ is the total hypothetical elastic strain energy. Next, the total strain energy that is vulnerable for redistribution due to plastic deformations U_{dist} is determined as

$$U_{\text{dist}} = \int_\Omega ((\sigma_{ij}\varepsilon_{ij})_{\text{hyp elastic}} - \sigma_y\varepsilon_y)_x\,\kappa_x\,dV, \qquad (37)$$

where $\kappa_x = 1$ if $((\sigma_{ij}\varepsilon_{ij})_{\text{hyp elastic}} - \sigma_y \varepsilon_y)_x > 0$, otherwise $\kappa_x = 0$ and σ_y is the uniaxial material yield strength. $\varepsilon_y = \sigma_y / E$, where E is the Young's modulus. The pseudo value of the material yield strength $\sigma_{y\ \text{pseudo}}$ is evaluated as follows

$$\frac{U_{\text{dist}}}{U_{\text{hyp elastic}}} \approx \frac{c(\sigma_y - \sigma_{y\ \text{pseudo}})}{\sigma_y}, \tag{38}$$

where c is a constant that depends on the geometry of the stress-strain curve.

3. Adaptive FEM-BEM Coupling Method

In this section we present an adaptive FEM-BEM coupling method for elasto-plastic analysis. The method is valid for both two- and three-dimensional applications. It estimates the FEM and BEM sub-domains and automatically generates/adapts the FEM and BEM meshes/sub-domains, according to the state of computation. The adaptive coupling method enhances those presented in [29,34,35] and improves the estimation of regions where plastic material behavior is going to develop (regions where the FEM is employed). In the presence of plastic deformations in the FEM region, the solution there is obtained via an iterative scheme. Naturally, an improvement to the estimated FEM and BEM sub-domains will result in additional savings of required system resources and/or a higher potential advantage of eliminating the cumbersome trial and error process in the identification of the FEM and BEM sub-domains. Materials of von-Mises type are considered in this investigation.

The basic steps of implementation of the proposed adaptive FEM-BEM coupling method may be summarized as follows (Figure 1):

1. Levels of loading $(LL_1, LL_2, ..., LL_i, ...LL_m)$ are specified by the user/analyst in order to get an estimate of the FEM and BEM sub-domains (LL_m is the maximum level of loading for the problem at hand).

   If the user/analyst prefers to use a constant interface throughout the FEM-BEM coupling analysis, the maximum load level LL_m is specified. Estimated FEM and BEM sub-domains will be utilized for all load increments.

2. For $k = 1,2,...,m$

2.1. A hypothetical elastic stress state is determined for the load level LL_k via BEM elastic analysis with initial BEM discretization or FEM elastic analysis utilizing a FEM coarse mesh.

2.2. Regions that violate the yield condition (utilizing the hypothetical elastic stresses of 2.1) are detected. A subsequent elastic analysis is conducted with "effective" material properties for the detected regions (effective Young's modulus $E_{k,eff}$ and Poisson ratio $\nu_{k,eff}$) and material properties E and ν for the remainder of the problem.

2.3. The hypothetical elastic state of stresses of step 2.2 is checked against a pseudo value of the material yield strength $\sigma_{y\,\text{pseudo}}$. FEM discretization is automatically generated for the regions that violate the pseudo yielding condition. It may be useful to add a few bands of finite elements around the perimeter of the discretized FEM sub-domain. Consequently, the BEM discretization is generated so as to represent best the remaining bounded/unbounded linear elastic regions (Figure 2).

2.4. Coupled FEM-BEM stress analysis involving elasto-plastic deformations is conducted for the current load increment.

2.5. A repetition of step 2.4 is required for the next load increment if the current state of computation in addition to the load increment is less than or equal to LL_k, else go to step 2.1.

It should be emphasized that steps 1-2.3 are carried out for the sole purpose of estimating and adapting the FEM and BEM sub-domains according to the state of computation. Effective material properties ($E_{k,eff}$ and $\nu_{k,eff}$) and the pseudo value of the material yield strength ($\sigma_{y\,\text{pseudo}}$) are not involved in carrying out step 2.4.

In the remainder of this section we will elaborate more on the determination of the pseudo value of the material yield strength ($\sigma_{y\,\text{pseudo}}$) and the effective material properties ($E_{k,eff}$ and $\nu_{k,eff}$) at a typical level of loading LL_k.

The simplicity of linear elastic analysis and the difficulties associated with non-linear elasto-plastic analysis have motivated some researchers to attempt solving elasto-plastic problems by adapting a modified form of available elastic solutions (see, e.g., references [36-42]). Linear elastic analysis in an iterative manner with a complete spatial distribution of updated material properties is conducted at each iteration in order to approximately

simulate elasto-plastic behavior. It is worth emphasizing that we are not interested over here in utilizing a similar approach for solving problems in elasto-plasticity. Our aim is to determine the regions that are sensible for FEM discretization. The schemes for updating the material properties include projection, arc length, and energy methods (Figure 3). Material points with the same stress level are represented by single points (e.g. a, b, e and f) on the uniaxial stress-strain curve (Figure 4).

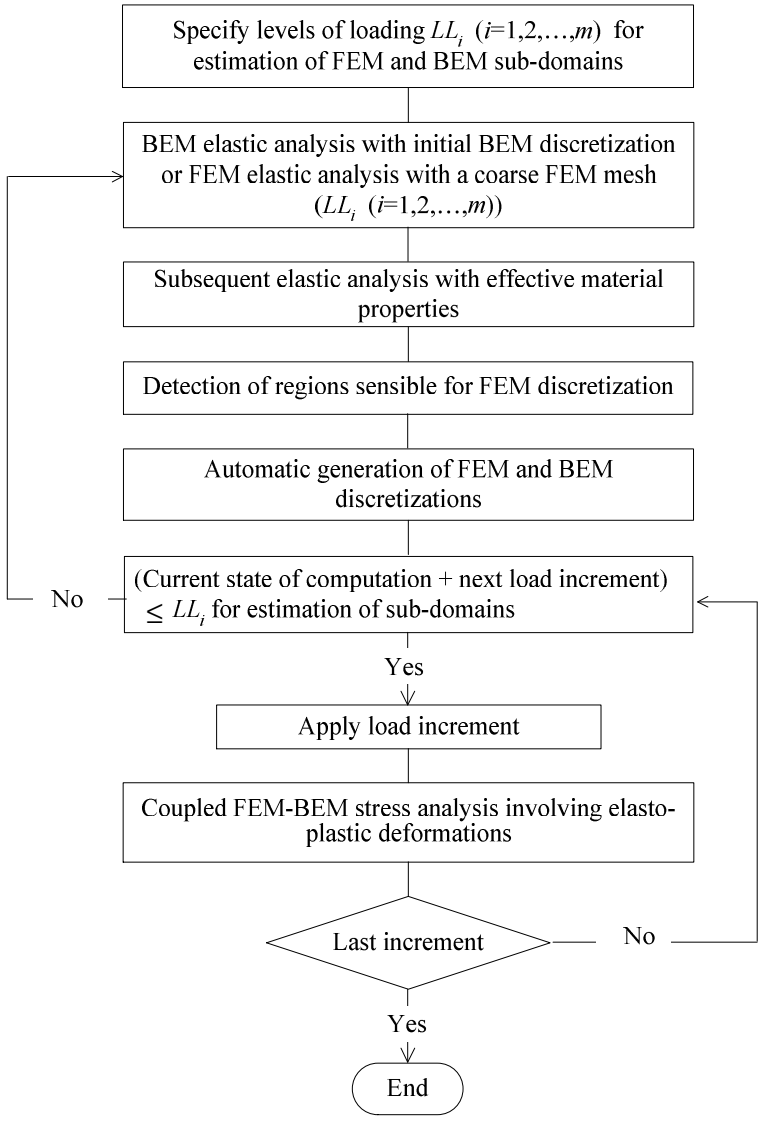

Figure 1: Adaptive FEM-BEM coupling method.

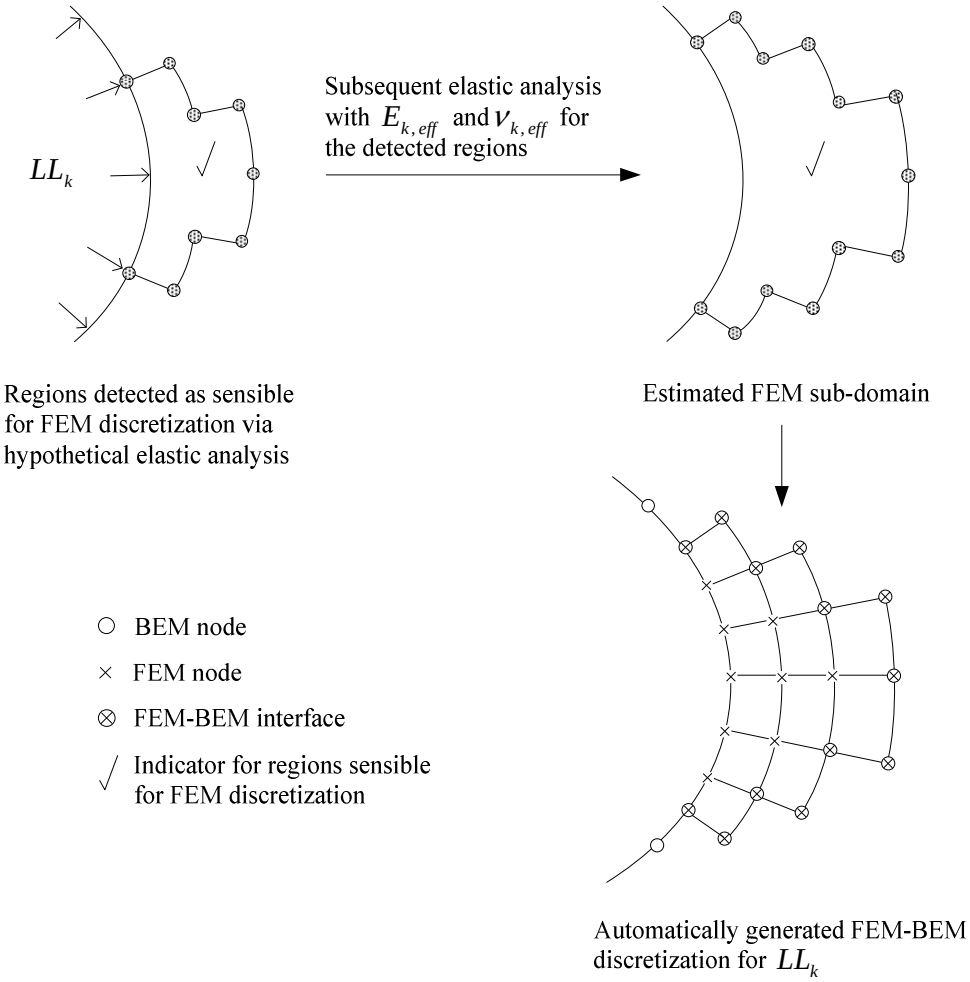

Figure 2: Estimated FEM and BEM sub-domains.

Let us consider materials of von-Mises type obeying a bilinear strain hardening rule. Neuber's and strain energy density methods (Figure 3) assume an energy balance between the strain energy density corresponding to the elasto-plastic stress-strain state and the hypothetical elastic strain energy density (same geometry submitted to the same loading [36-42]). For uni-dimensional states of stress, it is assumed that the product of stress and strain in elasticity is locally identical to the same product calculated by means of an elasto-plastic analysis. For tri-dimensional states of stress, the fundamental hypothesis may be written as [36-42]

$$(\sigma_{ij}\varepsilon_{ij})_{\text{elasto-plastic}} \cong (\sigma_{ij}\varepsilon_{ij})_{\text{hyp elastic}} \tag{39}$$

where $(.)_{\text{hyp elastic}}$ means a value determined from a hypothetical elastic computation for the stress (σ_{ij}) and the strain (ε_{ij}) tensors.

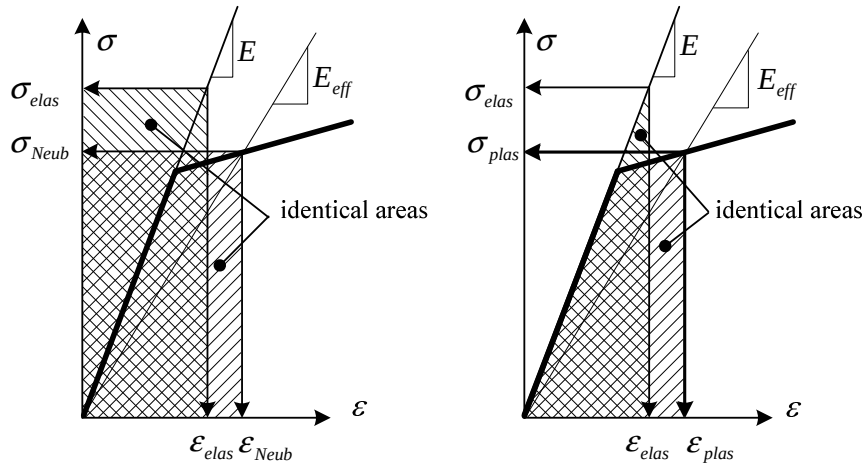

Figure 3: Energetic methods (Neuber's and strain energy density methods).

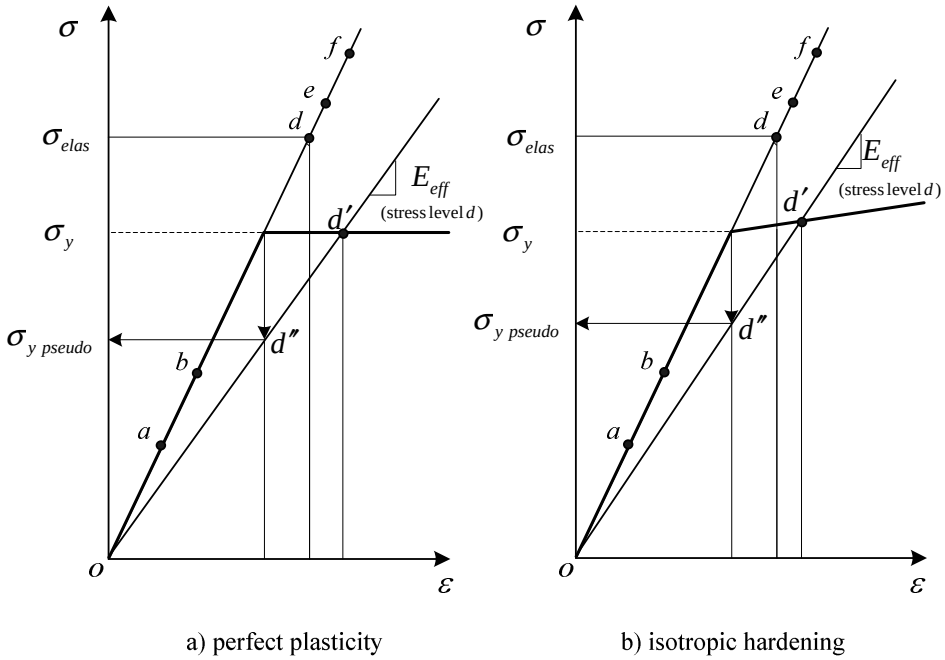

Figure 4: Effective Young's modulus and pseudo material yield strength.

From a virtual work principle we utilize the global formulation (Equation (36)). We further assume that there exists a stress level with which effective material properties are determined (stress level d, Figure 4). Next, at a typical level of loading LL_k we define the total strain energy that is vulnerable for redistribution due to plastic deformations $U_{k,\ \mathrm{dist}}$ as the total hypothetical strain energy of the regions that violate the yield condition (step 2.2, basic steps of implementation of the adaptive coupling method)

$$U_{k,\ \mathrm{dist}} = \int_{\Omega} ((\sigma_{ij}\varepsilon_{ij})_{\mathrm{hyp\ \ elastic}})_x \kappa_x dV, \tag{40}$$

where $\kappa_x = 1$ if $((\sigma_{ij}\varepsilon_{ij})_{\mathrm{hyp\ \ elastic}} - \sigma_y\varepsilon_y)_x > 0$, otherwise $\kappa_x = 0$.

The effective Young's modulus $E_{k,\ eff}$ is then evaluated (Figures 3,4) as follows

$$\frac{2(U_{k,\ \mathrm{hyp\ \ elastic}} - U_{k,\mathrm{dist}})}{2U_{k,\ \mathrm{hyp\ \ elastic}} - U_{k,\mathrm{dist}}} \approx \frac{2((\sigma_{ij}\varepsilon_{ij})_{\mathrm{hyp\ \ elastic}} - ((\sigma_{ij}\varepsilon_{ij})_{\mathrm{hyp\ \ elastic}} - \sigma_y\varepsilon_y))_{\mathrm{stress\ level\ d}}}{(2(\sigma_{ij}\varepsilon_{ij})_{\mathrm{hyp\ \ elastic}} - ((\sigma_{ij}\varepsilon_{ij})_{\mathrm{hyp\ \ elastic}} - \sigma_y\varepsilon_y))_{\mathrm{stress\ level\ d}}} = \frac{cE_{k,\,eff}}{E}, \tag{41}$$

where c is a constant. For perfect plasticity $c = 1$. For isotropic hardening plasticity models, it is concluded from Figure 4 that $c = 1$ is a conservative and at the same time reasonable value. The effective Poisson ratio $\nu_{k,\,eff}$ is obtained from equations adopted in iterative elastic analyses in order to simulate elasto-plastic behavior [36]

$$1/E_{k,\,eff} = 1/E + 2\phi_k/3 \tag{42}$$

and

$$\nu_{k,\,eff} = E_{eff}(\nu/E + \phi_k/3). \tag{43}$$

It should be emphasized over here that $E_{k,\,eff}$ and $\nu_{k,\,eff}$ may be calculated as constant values for the whole elastically predicted yielded region. Alternatively, a more accurate estimate of the FEM and BEM regions is obtained by calculating $E_{k,\,eff}$ and $\nu_{k,\,eff}$ for a finite number of equivalent stress levels (von Mises stresses). Then the regions with the same equivalent stresses (e.g., stress levels e and f, Figure 4) will be utilized to construct a finite number of layers with different material properties $E_{k,\,eff}$ and $\nu_{k,\,eff}$. Equations (41) through (43) are used in calculation of $E_{k,\,eff}$ and $\nu_{k,\,eff}$ for each layer (with the appropriate stress level). A subsequent elastic analysis (step 2.2, basic steps of implementation) is then conducted.

For the determination of the pseudo value of the material yield strength, we further investigate the uniaxial stress-strain curve. Relating the hypothetical elastic stress state

curve (stress level d, Figure 4) to that of the effective material parameters (stress level d'', Figure 4), it may be easily concluded that

$$\frac{2(U_{k,\ \text{hyp}\ \ \text{elastic}} - U_{k,\text{dist}})}{2U_{k,\ \text{hyp}\ \ \text{elastic}} - U_{k,\text{dist}}} \approx \frac{2((\sigma_{ij}\varepsilon_{ij})_{\text{hyp}\ \ \text{elastic}} - ((\sigma_{ij}\varepsilon_{ij})_{\text{hyp}\ \ \text{elastic}} - \sigma_y\varepsilon_y))_{\text{stress level d}}}{(2(\sigma_{ij}\varepsilon_{ij})_{\text{hyp}\ \ \text{elastic}} - ((\sigma_{ij}\varepsilon_{ij})_{\text{hyp}\ \ \text{elastic}} - \sigma_y\varepsilon_y))_{\text{stress level d}}} = \frac{c\sigma_{y\ \text{pseudo}}}{\sigma_y}. \tag{44}$$

Finally, the hypothetical elastic state of stresses (step 2.2, basic steps of implementation) is checked against yielding with the pseudo value of the material yield strength. Regions that violate the pseudo yielding condition are determined. An estimate of the FEM sub-domain is obtained. The procedure outlined with its inherent assumptions provides a simple, at the same time fast and effective, method for an estimate of the FEM and BEM sub-domains. A usual FEM-BEM coupling analysis is then conducted (step 2.4, basic steps of implementation) while utilizing the estimated FEM and BEM sub-domains.

Compared to the adaptive coupling method of [29,34,35], the presented method involves additional FEM or BEM elastic iterations. These elastic iterations involved in estimation of the FEM and BEM sub-domains are more than rewarded by an improved estimate of the FEM and BEM sub-domains provided by the proposed adaptive coupling method.

4. Example applications

In this section we present a number of two- and three- dimensional applications that highlight the effectiveness of the adaptive FEM-BEM coupling method presented in Section 3.

4.1 V-notched specimen

A specimen containing a sharp notch is analyzed in this example. The specimen is subjected to a tensile stress $P = 1.47015\text{x}10^6$ N/m^2. The geometry of the problem is shown in Figure 5 ($h = 0.036$ m and w = 0.02 m). The elastic material properties are described by Young's modulus ($E = 700\text{x}10^6$ N/m^2) and Poisson's ratio ($\nu = 0.2$). Material of von-Mises type is considered ($\sigma_y = 2.43\text{x}10^6$ N/m^2), with no hardening effect ($H = 0$), as a yield function and plane strain loading conditions. Due to symmetry, only one quarter of the specimen is modeled.

The problem is solved by means of the adaptive coupling method presented in Section 3. Figure 6 shows the estimate of the regions sensible for discretization by the FEM. The FEM discretization is generated over those regions, while the BEM mesh is generated to

represent the remaining linear elastic region (steps 1-2.3, basic steps of implementation, Section 3). A coupled FEM-BEM stress analysis is then conducted (step 2.4, basic steps of implementation, Section 3). For this example and without loss of generality, we choose the conventional (direct) approach for the coupling of the FEM and BEM discretized system of equations (Section 2.3). A coupled FEM-BEM computer code has been developed for the elasto-plastic analysis using the ideas presented in Section 2 (conventional coupling) and Section 3 (estimation of FEM and BEM sub-domains, automatic generation and progressive adaption of the FEM and BEM meshes/sub-domain). We utilize some parts of a code originally developed by the first author (two-dimensional FEM elasto-plastic analysis) for calculation of the FEM matrices and a symmetric Galerkin boundary element computer code originally developed by O. Steinbach (see, e.g., reference [51]) for calculation of the BEM matrices.

The coupled FEM-BEM solutions are obtained with the automatically generated FEM and BEM meshes. Figure 6 shows the yielded regions obtained using the adaptive coupled FEM-BEM method. The results clearly show that the adaptive FEM-BEM coupled method employs smaller FEM sub-domains. Moreover, the method is practically advantageous as it does not necessitate the predefinition and manual localization of the FEM and BEM sub-domains.

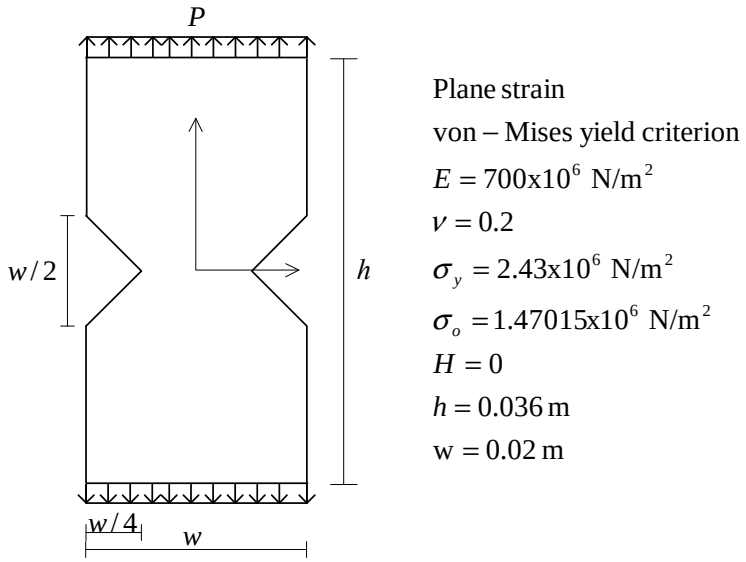

Figure 5: V-notched specimen.

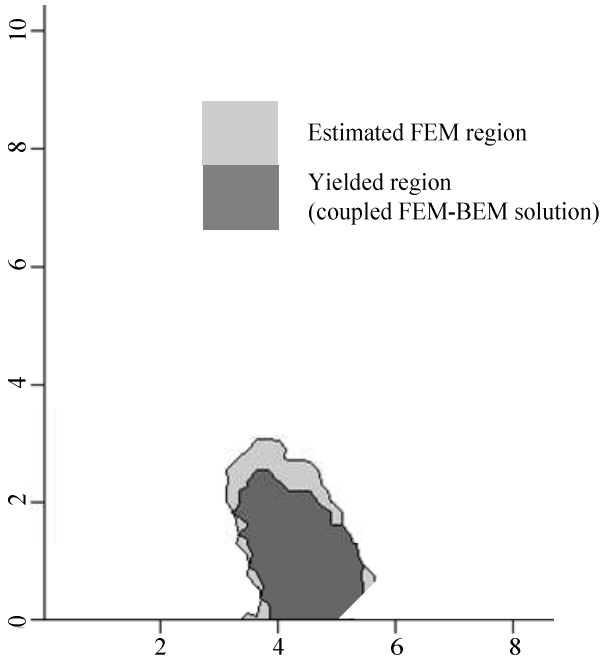

Figure 6: Estimated FEM region and yielded region (adaptive FEM-BEM coupling) for selected values of λ (example 4.1).

4.2 Square plate with a central elliptical defect

The second example is a square plate with a centered elliptical defect (Figure 7). The plate is subjected to uniformly distributed tensile loads over the two pairs of the opposing ends (equal biaxaial tension). The applied tractions $P = 100 \text{ x} 10^6 \text{ N/m}^2$ are scaled with a load factor λ. The elastic material properties of the plate are described by Young's modulus ($E = 206.9\text{x}10^9 \text{ N/m}^2$) and Poisson's ratio ($\nu = 0.29$). Material of von-Mises type is considered ($\sigma_y = 450\text{x}10^6 \text{ N/m}^2$), with no hardening effect ($H = 0$), as a yield function and plane strain loading conditions. Due to symmetry, only one quarter of the plate is modeled.

Similar to the V-notch example (Section 4.1), the problem is solved by means of the adaptive coupling method presented in Section 3. The loads are applied incrementally. Estimates of the regions sensible for discretization by the FEM are obtained and the FEM mesh is generated over those regions. The BEM mesh is generated to represent the remaining linear elastic region (steps 1-2.3, basic steps of implementation, Section 3). The coupled FEM-BEM solutions (step 2.4, basic steps of implementation, Section 3) are

obtained with the automatically generated FEM and BEM discretization for particular values of λ (see Section 4.1 for details on the computer code utilized). Figure 8 additionally shows the yielded regions obtained using the adaptive coupled FEM-BEM method for the selected values of λ. Again the results clearly show the effectiveness and practicality of the adaptive coupling method.

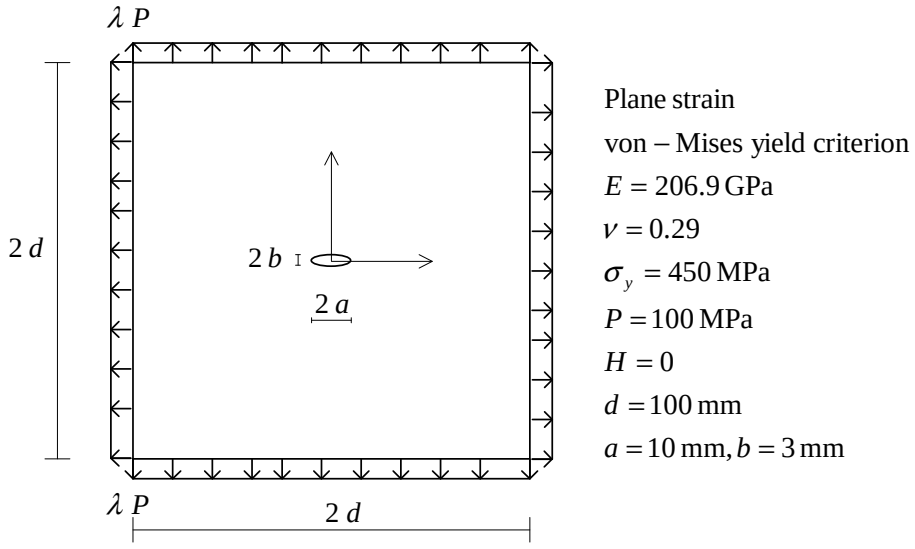

Figure 7: Plate with a centered elliptical defect.

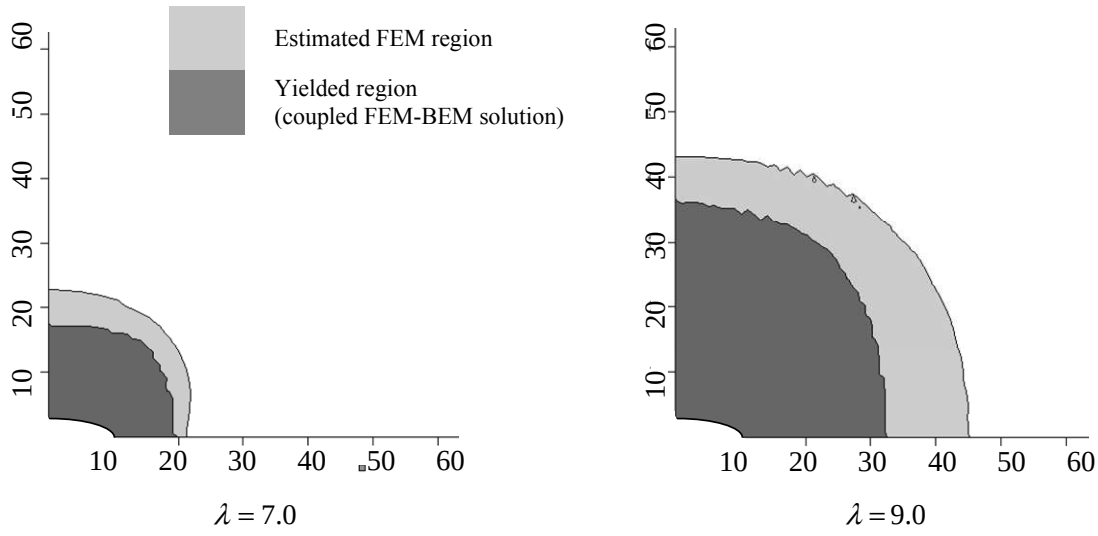

Figure 8: Estimated FEM region and yielded region (adaptive FEM-BEM coupling) for selected values of λ (example 4.2).

4.3 Three-dimensional plate with a central hole

The third example application (Figure 9) is a benchmark problem in computational plasticity [56]. The benchmark problem is a stretched steel plate ($b = h = 0.1$ m and $t = 0.01$ m) with a cylindrical central hole ($r = 0.01$ m). A surface load P is applied to the plate's upper and lower edges. The applied tractions $\mathrm{P} = 100\ \mathrm{x}10^6$ N/m^2 are scaled with the load factor λ. We keep the material properties of the previous example. Due to symmetry, only half quarter of the plate is modeled (Figure 9).

The loads are applied incrementally. Figure 10 shows the estimates of the FEM and BEM regions and the FEM and BEM discretizations. The FEM discretization is generated over the regions that are estimated as sensible for FEM discretization, while the BEM mesh is generated to represent the remaining linear elastic region (steps 1-2.3, basic steps of implementation, Section 3). The coupled FEM-BEM (step 2.4, basic steps of implementation, Section 3) solutions are obtained with the automatically generated FEM and BEM discretization for the particular values of λ. For this example, we choose the interface relaxation approach for the coupling of the FEM and BEM discretized system of equations (Section 2.3). We utilized the Finite Element Analysis Program (FEAP) for the FEM sub-domain computations [57] and the H-matrix ACA accelerated Galerkin BEM solver for the BEM sub-domain computations (see Section 2.1 and reference [43]).

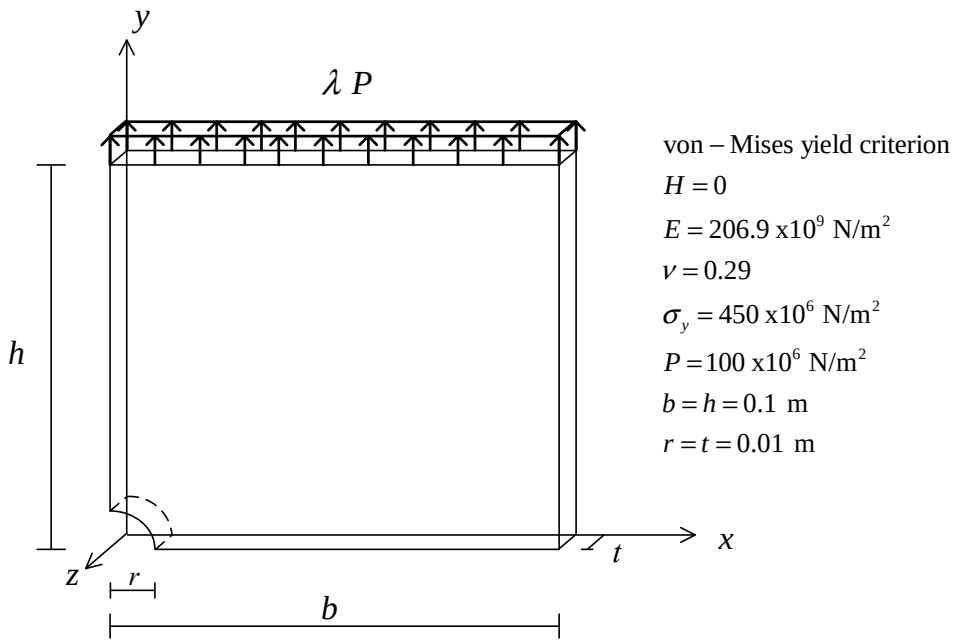

Figure 9: Three-dimensional plate with a central hole.

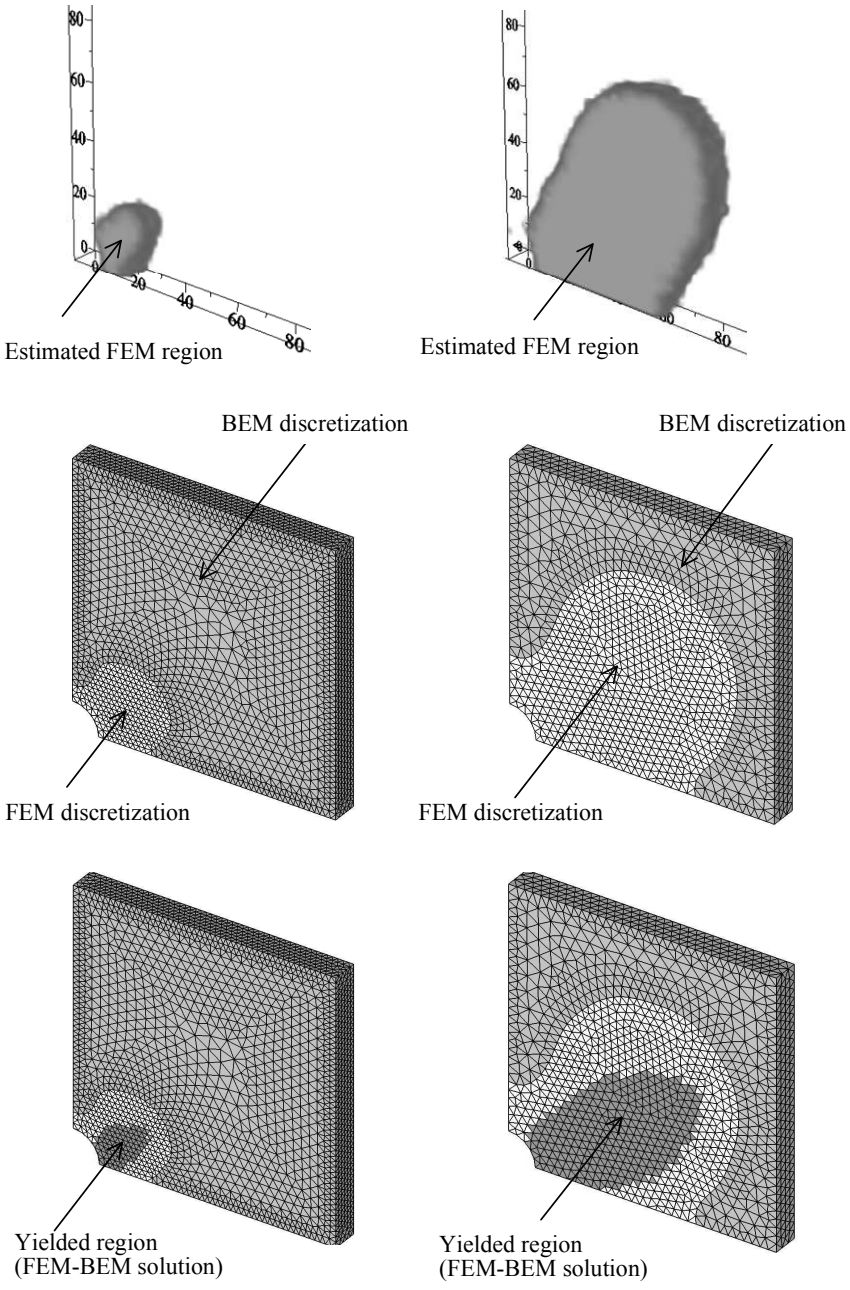

Figure 10: Estimated FEM region, FEM and BEM discretizations and yielded region (adaptive FEM-BEM) for selected values of λ (example 4.3).

Figure 10 shows the yielded regions obtained using the adaptive coupled FEM-BEM method for the selected values of λ. The computed results obtained using the adaptive FEM-BEM coupling method compare well with the reference solutions [56]. Figure 9 clearly show the effectiveness (the method employs smaller FEM sub-domains) and the practicality of the adaptive FEM-BEM coupling method (the method does not necessitate the predefinition and manual localization of the FEM and BEM sub-domains).

Conclusions

The present adaptive coupling method is practically advantageous as it does not necessitate predefinition and manual localization of the FEM and BEM sub-domains. Moreover, the method is computationally efficient as it substantially decreases the size of FEM meshes, which plainly leads to reduction of required system resources and gain in efficiency. The numerical results in two- and three- dimensional elasto-plastic analyses confirm the effectiveness of the proposed method.

References

[1.] Zienkiewicz, O. C., Kelly, D. M., and Bettes, P., "The Coupling of the Finite Element Method and Boundary Solution Procedures," *International Journal for Numerical Methods in Engineering*, Vol. 11, 1977, pp. 355-375.

[2.] Zienkiewicz, O. C., Kelly D. M., and Bettes P., "Marriage a la mode - the best of both worlds (Finite elements and boundary integrals)," in Energy Methods in Finite Element Analysis, Chapter 5, Glowinski, R., Rodin, E. Y. and Zienkiewicz O. C. (eds), Wiley, London, 1979, pp. 81–106.

[3.] Costabel, M., "Symmetric methods for the coupling of finite elements and boundary elements," In Boundary Elements IX, Brebbia, C., Wendland, W. and Kuhn, G. (eds.), Springer, Berlin, Heidelberg, New York, 1987, pp. 411–420.

[4.] Costabel, M. and Stephan, E. P., "Coupling of Finite and Boundary Element Methods for an Elastoplastic Interface Problem," *SIAM Journal on Numerical Analysis*, Vol. 27, Issue 5, 1990, pp. 1212-1226.

[5.] Holzer, S. M., "Das Symmetrische Randelementverfahren: Numerische Realisierung und Kopplung mit der Finite-Elemente-Methode zur Elastoplastischen Strukturanalyse," Technische Universität München, Munich, 1992.

[6.] Anonymous, "State of the Art in BEM/FEM Coupling," *Boundary Elements Communications*, Vol. 4, 1993, pp. 58-67.

[7.] Anonymous, “State of the Art in BEM/FEM Coupling,” *Boundary Element Methods Communications*, Vol. 4, 1993, pp. 94-104.

[8.] Polizotto, C. and Zito, M., “Variational Formulations for Coupled BE/FE methods in Elastostatics,” *ZAMM*, Vol. 74, Issue 11, 1994, pp. 553-543.

[9.] Langer, U., “Parallel Iterative Solution of Symmetric Coupled FE/BE-Equation via Domain Decomposition,” *Contemporary Mathematics*, vol. 157, 1994, pp. 335-344.

[10.] Brink, U., Klaas, O., Niekamp, R. and Stein, E., “Coupling of Adaptively Refined Dual Mixed Finite Elements and Boundary Elements in Linear Elasticity,” *Advances in Engineering Software*, Vol. 24, Issues 1-3, 1995, pp. 13-26.

[11.] Carstensen, C., Zarrabi, D. and Stephan, E. P., “On the h-Adaptive Coupling of FE and BE for Viscoplastic and Elasto-Plastic Interface Problems,” *Journal of Computational and Applied Mathematics*, Vol. 75, Issue 2, 1996, pp. 345-363.

[12.] Carstensen, C., “On the Symmetric Boundary Element Method and the Symmetric Coupling of Boundary Elements and Finite Elements,” IMA Journal of Numerical Analysis, Vol. 17, No. 2, 1997, pp. 201-208.

[13.] Haase, G., Heise, B., Kuhn, M., and Langer, U., “Adaptive Domain Decomposition Methods for Finite and Boundary Element Equations,” In Boundary Element Topics, Wendland, W. (ed.), Berlin, 1998. Springer-Verlag, 1998, pp. 121-147.

[14.] Mund, P. and Stephan, P., “An Adaptive Two-Level Method for the Coupling of Nonlinear FEM-BEM Equations,” *SIAM Journal on Numerical Analysis*, Vol. 36, No. 4, 1999, pp. 1001-1021.

[15.] Ganguly S, Layton J. B. and Balakrishma, C., "Symmetric Coupling of Multi-Zone Curved Galerkin Boundary Elements with Finite Elements in Elasticity," *International Journal of Numerical Methods in Engineering*, Vol. 48, 2000, pp. 633-654.

[16.] Elleithy, W. M., Al-Gahtani, H. J. and El-Gebeily, M., "Iterative Coupling of BE and FE Methods in Elastostatics," *Engineering Analysis with Boundary Elements*, Vol. 25, Issue 8, 2001, pp. 685-695.

[17.] El-Gebeily, M., Elleithy, W. M. and Al-Gahtani, H. J., "Convergence of the Domain Decomposition Finite Element-Boundary Element Coupling Methods," *Computer Methods in Applied Mechanics and Engineering*, Vol. 191, Issue 43, 2002, pp. 4851-4867.

[18.] Gaul, L. and Wenzel, W., “A Coupled Symmetric BE–FE Method for Acoustic Fluid–Structure Interaction,” *Engineering Analysis with Boundary Elements*, Vol. 26, Issue 7, 2002, pp. 629-636.

[19.] Hass, M. and Kuhn, G., “Mixed-Dimensional, Symmetric Coupling of FEM and BEM,” *Engineering Analysis with Boundary Elements*, Vol. 27, Issue 6, June 2003, Pages 575-582.

[20.] Langer, U. and Steinbach, O., “Coupled Boundary and Finite Element Tearing and Interconnecting Methods,” Proceedings of the Fifteenth International Conference on Domain Decomposition, Berlin, Germany, July 2003, pp. 83-98.

[21.] Elleithy, W. M. and Tanaka, M., “Interface Relaxation Algorithms for BEM-BEM Coupling and FEM-BEM Coupling,” *Computer Methods in Applied Mechanics and Engineering*, Vol. 192, Issue 26-27, 2003, pp. 2977-2992.

[22.] Stephan, E. P., “Coupling of Boundary Element Methods and Finite Element Methods,” Encyclopedia of Computational Mechanics, Vol. 1 Fundamentals, Chapter 13, Stein, E., de Borst, R. and Hughes, T. J. R. (eds.), John Wiley & Sons, Chichester, 2004, pp. 375-412.

[23.] Elleithy, W. M. and Tanaka, M. and Guzik, A., “Interface Relaxation FEM-BEM Coupling Method for Elasto-Plastic Analysis,” *Engineering Analysis with Boundary Elements*, Vol. 28, Issue 7, June 2004, pp. 849-857.

[24.] Von Estorff, O. and Hagen, C., “Iterative coupling of FEM and BEM in 3D transient elastodynamics,” *Engineering Analysis with Boundary Elements*, Vol. 29, Issue 8, 2005, pp. 775-787.

[25.] Soares, Jr. D., von Estorff, O. and Mansur, W. J., "Efficient Nonlinear Solid-Fluid Interaction Analysis by an Iterative BEM/FEM Coupling,“ *International Journal for Numerical Methods in Engineering*, Vol. 64, Issue 11, 2005, pp. 1416-1431.

[26.] Haas, M., Helldörfer, B. and Kuhn, G., “Improved Coupling of Finite Shell Elements and 3D Boundary Elements,” *Archive of Applied Mechanics*, Vol. 75, 2006, pp. 649-663.

[27.] Springhetti, R., Novati, G. and Margonari, M., "Weak Coupling of the Symmetric Galerkin BEM with FEM for Potential and Elastostatic Problems", *Computer Modeling in Engineering & Sciences*, Vol. 13, 2006, pp. 67-80.

[28.] Chernov, A., Geyn, S., Maischak, M. and Stephan, E. P., “Finite Element/Boundary Element Coupling for Two-Body Elastoplastic Contact Problems with Friction,” in:

Analysis and Simulation of Contact Problems, Wriggers, P. and Nackenhorst, U. (eds.), Lecture Notes in Applied and Computational Mechanics, Vol. 27, 2006, pp. 171-178.

[29.] Elleithy, W., "Analysis of Problems in Elasto-Plasticity via an Adaptive FEM-BEM Coupling Method," *Computer Methods in Applied Mechanics and Engineering*, Vol. 197, Issues 45-48, August 2008, pp. 3687-3701.

[30.] Astrinidis, E., Fenner, R. T. and Tsamasphyros, G., "Elastoplastic Analysis with Adaptive Boundary Element Method," *Computational Mechanics*, Vol. 33, No. 3, 2004, pp. 186-193.

[31.] Maischak, M. and Stephan, E. P., "Adaptive *hp*-Versions of Boundary Element Methods for Elastic Contact Problems," *Computational Mechanics*, Vol. 39, No. 5, 2007, pp. 597-607.

[32.] Doherty, J. P. and Deeks, A. J., "Adaptive Coupling of the Finite-Element and Scaled Boundary Finite-Element Methods for Non-Linear Analysis of Unbounded Media," *Computers and Geotechnics*, Vol. 32, Issue 6, 2005, pp. 436-444.

[33.] Ribeiro, T. S. A., Beer, G. and Duenser, C., "Efficient elastoplastic analysis with the boundary element method," Computational Mechanics, Vol. 41, No. 5, 2008, pp. 715-732.

[34.] Elleithy, W. and Langer, U., "Adaptive FEM-BEM Coupling Method for Elasto-Plastic Analysis," Eighth International Conference on Boundary Element Techniques (BeTeq 2007), Naples, Italy, July 2007, pp. 269-274.

[35.] Elleithy, W. and Langer, U., "Efficient Elasto-Plastic Analysis via an Adaptive Finite Element–Boundary Element Coupling Method," Thirtieth International Conference on Boundary Elements and Other Mesh Reduction Methods (BEM/MRM XXX), Maribor, Slovenia, July 2008, pp. 229-238.

[36.] Jahed, H., Sethuraman, R. and Dubey, R. N., "A Variable Material Property Approach for Solving Elasto-Plastic Problems," *International Journal of Pressure Vessels and Piping*, Vol. 71, Issue 3, pp. 285-291, 1997.

[37.] Desikan, V. Sethuraman, R., "Analysis of Material Nonlinear Problems using Pseudo-Elastic Finite Element Method," *ASME Journal of Pressure Vessel Technology*, ASME, Vol. 122, 2000, pp. 457-461.

[38.] Ponter A. R. S., Fuschi P. and Engelhardt M., "Limit Analysis for a General Class of Yield Conditions," *European Journal of Mechanics A-Solids*, Vol. 19, No. 3, 2000, pp. 401-422.

[39.] Desmorat, R., "Fast Estimation of Localized Plasticity and Damage by Energetic Methods," *International Journal of Solids and Structures*, Vol. 39, 2002, pp. 3289-3310.

[40.] Upadrasta, M., Peddieson, J., and Buchanan, G., "Elastic Compensation Simulation of Elastic/Plastic Axisymmetric Circular Plate Bending Using a Deformation Model," *International Journal of Non-Linear Mechanics*, Vol. 41, 2006, pp. 377-387.

[41.] Seshadri, R., "The Generalized Local Stress Strain (GLOSS) Analysis – Theory and Applications," *ASME Journal of Pressure Vessels Technology*, Vol. 113, 1991, pp. 219-227.

[42.] Mohamed, A., Megahed, M., Bayoumi, L. and Younan, M., "Application of Iterative Elastic Techniques for Elastic-Plastic Analysis of Pressure Vessels," *ASME Journal of Pressure Vessels Technology*, Vol. 121, 1999, pp. 24-29.

[43.] Bebendorf, M. and Grzhibovskis, R., "Accelerating Galerkin BEM for Linear Elasticity using Adaptive Cross Approximation," Mathematical Methods in the Applied Sciences, Vol. 29 Issue 14, 2006, pp. 1721-1747.

[44.] Rjasanow, S. and Steinbach, O., The Fast Solution of Boundary Integral Equations, Springer, 2007.

[45.] Sirtori, S., "General Stress Analysis Method by means of Integral Equations and Boundary Elements," *Meccanica*, Vol. 14, 1979, pp. 210-218.

[46.] Costabel, M. and Stephan, E. P., "Integral Equations for Transmission Problems in Linear Elasticity," *Journal of Integral Equations*, Vol. 2, 1990, pp. 211-223.

[47.] Sirtori, S., Maier, G., Novati, G. and Miccoli, S., "A Galerkin Symmetric Boundary Element Method in Elasticity: Formulation and Implementation," *International Journal for Numerical Methods in Engineering*, Vol. 35, 1992, pp. 255-282.

[48.] Bonnet, M., "Regularized Direct and Indirect Symmetric Variational BIE Formulations for Three-Dimensional Elasticity," *Engineering Analysis with Boundary Elements*, Vol. 15, Issue 1, 1995, pp. 93-102.

[49.] Bonnet, M., Maier, G. and Polizzotto, C., "Symmetric Galerkin Boundary Element Method," *Applied Mechanical Review*, Vol. 51, No. 11, 1998, pp. 669-704.

[50.] Steinbach, O., “Fast Solution Techniques for the Symmetric Boundary Element Method in Linear Elasticity,” *Computer Methods in Applied Mechanics and Engineering*, Vol. 157, 1998, pp. 185-191.

[51.] Of, G., Steinbach, O. and Wendland, W. L., “Application of a Fast Multipole Galerkin in Boundary Element Method in Linear Elastostatics,” *Computing and Visualization in Science*, Vol. 8, No. 3-4, December 2005, pp. 201-209.

[52.] Kupradze, V., Three-Dimensional Problems of the Mathematical Theory of Elasticity and Thermoelasticity, North-Holland Series in Applied Mathematics and Mechanics, North-Holland, Amsterdam, 1979.

[53.] Owen, D. R. J. and Hinton, E., Finite Elements in Plasticity: Theory and Practice, Pineridge Press, Swansea, U.K., 1980.

[54.] Simo, J. C. and Hughes, T. J. R., Computational Inelasticity, Springer, 1998.

[55.] Elleithy, W., “Interface Relaxation FEM-BEM Coupling: Dynamic Procedures of Determining the Relaxation Parameters,” Sixth Alexandria International Conference on Structural and Geotechnical Engineering (AICSGE6), Alexandria, Egypt, April 2007, pp. ST1-ST15.

[56.] Stein, E., Wriggers, P., Rieger, A. and Schmidt, M., “Benchmarks,” In Error-Controlled Adaptive Finite Elements in Solid Mechanics, E. Stein (ed.), 2003, Wiley, pp. 385-404.

[57.] Taylor, R. L., FEAP - A Finite Element Analysis Program, Version 8.2, Theory Manual, University of California at Berkeley, 2008.